Article

Not peer-reviewed version

Lightweight Knee Orthosis for Athletic Rehabilitation: Achieving 40% Weight Reduction with Topology Optimization in Generative AI Design

Hong Yi Goh , Xianlong Zhang , Wei En Ley , Zhen Bin It * , Jovan Bowen Heng , Tee Hui Teo

Posted Date: 10 July 2025

doi: 10.20944/preprints202507.0892.v1

Keywords: generative AI

 doi:10.20944/preprints202507.0892.v1

Article

Lightweight Knee Orthosis for Athletic Rehabilitation: Achieving 40% Weight Reduction with Topology Optimization in Generative AI Design

Hong Yi Goh [1], Xianlong Zhang [1], Wei En Ley [1], Zhen Bin It [2], Jovan Bowen Heng [2] and Tee Hui Teo [2,*]

[1] The University of Newcastle, Callaghan, 2308, Australia
[2] Singapore University of Technology and Design, Singapore
* Correspondence: tthui@sutd.edu.sg

Abstract

The increasing demand for lightweight and cost-efficient orthopedic support in sports rehabilitation has accelerated the adoption of AI-driven design methodologies. This proposed work demonstrates the novelty of applying topology optimization within the Functional Generative Design (FGD) module of the 3DExperience platform to develop a structurally optimized knee orthosis. Under mixed mass constraints, the initially optimized thigh and shin brace designs achieved 51-gram and 62-gram weight reductions respectively while maintaining mechanical integrity under a 5000N physiological load. Finite element analysis revealed a 23 MPa reduction in Von Mises stress compared to the 50% mass design, indicating improved stress distribution. The final prototype braces, chosen with mass constraints of 45% and 50% for the thigh and shin respectively, 3D-printed using Polylactic Acid (PLA), were tested on a user's leg and showed good anatomical fit, flexibility, and comfort, while achieving a combined final weight reduction of 122-grams (40%) compared to the original model. These improvements enhance wearer mobility while reducing material use and production cost.

Keywords: generative AI

1. Introduction

This proposed work focuses on developing a lightweight and customizable knee orthosis tailored for general rehabilitation and athletic recovery using Functional Generative Design (FGD) on the 3DExperience platform. Traditional off-the-shelf knee braces often lack personalization, leading to bulky and uncomfortable products that can hinder usability and cost-efficiency. By leveraging recent advancements in generative design and additive manufacturing, this study aims to create a structurally optimized, user-friendly brace through iterative simulations, prototyping, and refinement. Although anatomical data was collected using 3D scanning, the design was intentionally generalized to test broader usability beyond a single user's profile, enhancing its application in diverse rehabilitation settings. Incorporating clinical insights, the design process aligns with evidence-based recovery benchmarks, particularly targeting a knee flexion range within the first month post-surgery. This parameter serves as a design requirement for the hinge mechanism to ensure sufficient early-stage support. Beyond the technical development, the proposed work showcases how engineering, healthcare, and digital manufacturing intersect to offer scalable, personalized solutions in orthopedic care.

 doi:10.20944/preprints202507.0892.v1

2. Literature Review

Generative design and topology optimization are increasingly used to develop orthotic devices that minimize weight while maintaining structural integrity. In biomedical applications, these methods enable the creation of complex, material-efficient geometries without compromising strength or functionality. Custom wrist splints validated by finite element analysis have achieved high motion restriction with low discomfort, supporting dynamic rehabilitation [1]. In prosthetic foot design, compliant mechanisms replicate natural gait through controlled deformation, reducing material usage compared to rigid structures [2]. Lattice-optimized brace shells balance support and airflow, enhancing long-duration comfort [3], while anatomically tailored prosthetic sockets improve stress distribution using CATIA-based topology workflows [4]. Algorithmic refinement of lattice structures enables designers to trade stiffness for reduced weight, improving personalization and fatigue resistance [5]. Simulation-driven optimization integrated into CAD platforms has further refined jointed ankle supports by directly incorporating gait mechanics [6]. Collectively, these approaches can reduce material usage by up to 50% while preserving structural performance, making them well-suited for lightweight athletic orthoses. Lower-limb orthoses must accommodate biomechanical loads and dynamic gait patterns. Studies have shown that intentional hinge misalignments in braces can alter joint kinematics but may not always reduce ligament strain, emphasizing the importance of anatomical alignment [7]. Valgus and external rotation configurations, especially when combined with lateral wedge foot orthoses, significantly reduce medial knee loading and improve comfort [8]. However, excessive rigidity in ankle-foot orthoses can suppress muscle activation, potentially hindering gait retraining and neuromuscular recovery [9]. Community programs using 3D-printed assistive orthoses have reported improvements in gait speed and user confidence, validating the role of adaptable structural design [10]. Improper strapping or misalignment during donning remains a critical failure point, often negating intended biomechanical benefits [6]. Postoperative studies on knee flexion after total knee arthroplasty (TKA) identified one-month flexion as a strong predictor of long-term recovery, with 105° at one month serving as the optimal benchmark for achieving 120° at 12 months [11]. Based on this, the target range of motion for this study was defined around 105° flexion, informing the hinge range of motion specifications. Aligning the design objectives with clinical recovery benchmarks ensures that the prototype provides effective structural support during early rehabilitation.

2.1. Methodology

The design process began with an initial attempt to import a 3D-scanned human leg model into the Functional Generative Design environment on the 3DExperience platform. However, due to limitations in handling complex mesh data, manual measurements were instead used to approximate the lower limb geometry. A semi-circular support structure was designed for the thigh and shin, combined with adjustable velcro straps to accommodate varying leg sizes. Critical design regions such as strap holes, bolt holes, and hinge connectors were preserved using partitioning tools, while the remaining areas were left open for material optimization to improve weight-to-strength performance. Once the design regions were defined, preserved zones and bolt connections were specified to ensure structural continuity during optimization. Structural loads simulating knee flexion forces were applied to the outer surface, while fixed constraints were assigned to the velcro-strap areas. Directional restraints controlled unwanted movement, and a mesh was generated to validate stress and deformation. Optimization parameters included a mesh size of 3.3mm with a minimum thickness control of 10mm, and symmetry enforcement to ensure durability and manufacturability. After defining a mass constraint, the topology optimization was executed, iteratively removing material until an optimal design balancing stiffness, weight, and form was achieved. The mechanical properties of PLA were applied in the simulations to determine its applicability for 3D-printing [12]. Base designs of a thigh and shin brace with connecting stems were first created in Figure 1, with original masses of 0.131kg and 0.199kg respectively.

 doi:10.20944/preprints202507.0892.v1

The finalized digital designs were fabricated by 3D-printing with PLA. The use of additive manufacturing allowed for rapid iteration, particularly given the complex geometries resulting from topology optimization. While the generative forms were lightweight and efficient, printability challenges arose with thin overhangs and intricate interior cavities, requiring strategic support structures and orientation adjustments. Physical prototypes were tested on a user's leg to assess fit, comfort, and alignment, validating the practical application of the design and informing future refinements.

2.2. Design Results

The shin and thigh components were designed with functional constraints to optimize weight, fit, and flexibility. Shin design focused on accommodating muscle expansion and ease of adjustment, using velcro strap holes and an open posterior. The thigh brace followed a semi-cylindrical shape to offer stable support while allowing leg movement. Both designs were connected by rotational hinges, engineered to support natural knee flexion using bolt-secured connectors. After the basic models were created, topology optimization was performed with defined cutting values (75 for shin, 70 for thigh) to remove unnecessary material while maintaining structural integrity. Simulation results showed significant stress reduction in optimized models, particularly in high-stress areas like strap holes. Experiments involved a remote force of 5000N being applied normally to the brace's surface, shown in Figure 1 as green vectors, to simulate and assess the physical stresses exerted on a brace. The Von Mises stress results experienced by the braces were also shown in Figure 1, with the maximum displacements for both braces used in a comparative analysis in Table 1.

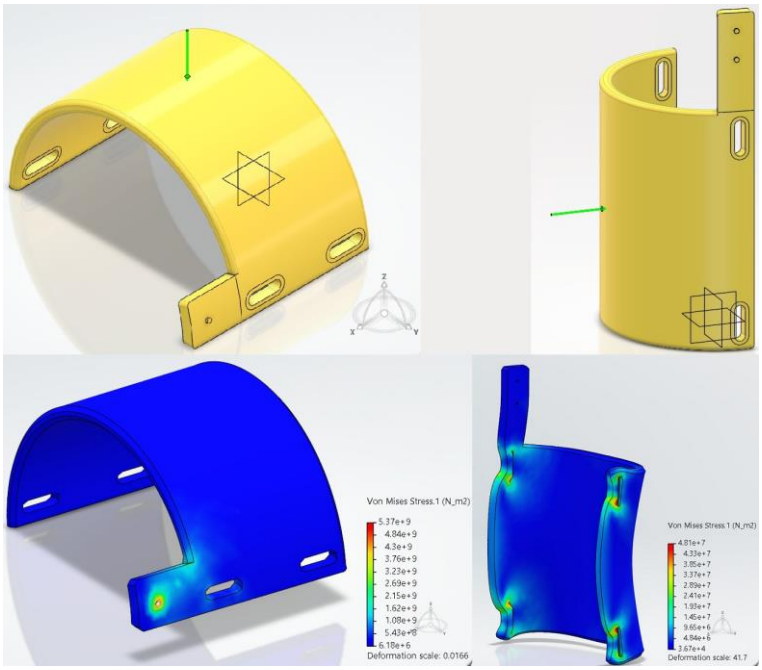

Figure 1. The upper section displays the base models of the thigh (left) and shin (right) brace. The visible green vectors were used for loading simulations, with Von Mises stress results shown in the lower section of the figure for both models.

From Equation 1, The Von Mises stress σ_v provides an equivalent stress value that indicates whether a ductile material (PLA in this context) reaches the yield strength σ_y of the material under complex loading conditions.

$$\sigma_v = \sqrt{\frac{1}{2}[(\sigma_x - \sigma_y)^2 + (\sigma_y - \sigma_z)^2 + (\sigma_z - \sigma_x)^2] + 3(\tau^2_{xy} + \tau^2_{yz} + \tau^2_{zx})} \quad (1)$$

The simulations performed on the base model produced Von Mises stress values that remained within the safe limits of PLA's mechanical capacity, with peak stresses observed at the velcro strap

 doi:10.20944/preprints202507.0892.v1

holes. The low stress values observed at the point of impact during the structural simulation indicated that the brace was able to evenly distribute the force around its entire frame, and did not exceed the typical yield strength of PLA [13]. This confirmed that under expected load conditions, the brace would not undergo plastic deformations or structural failure. The maximum stress can be shown in the four strap holes as the colour around the area is red and yellow. While the rest of the thigh design area experiences less stress. It is due to less reaction forces applying on the surface area when the user is wearing it to move around. Figure 2 illustrates the conceptual shapes of the shin and thigh designs, optimized through selective material removal. A cutting value of 70 was applied to the shin to define a clearer yet structurally valid shape, balancing weight reduction with integrity. For the slightly shorter thigh brace, a cutting value of 65 was used to preserve critical structural paths while minimizing excess material. Both thresholds produced lightweight, stable forms suitable for further analysis and prototyping without compromising functional support.

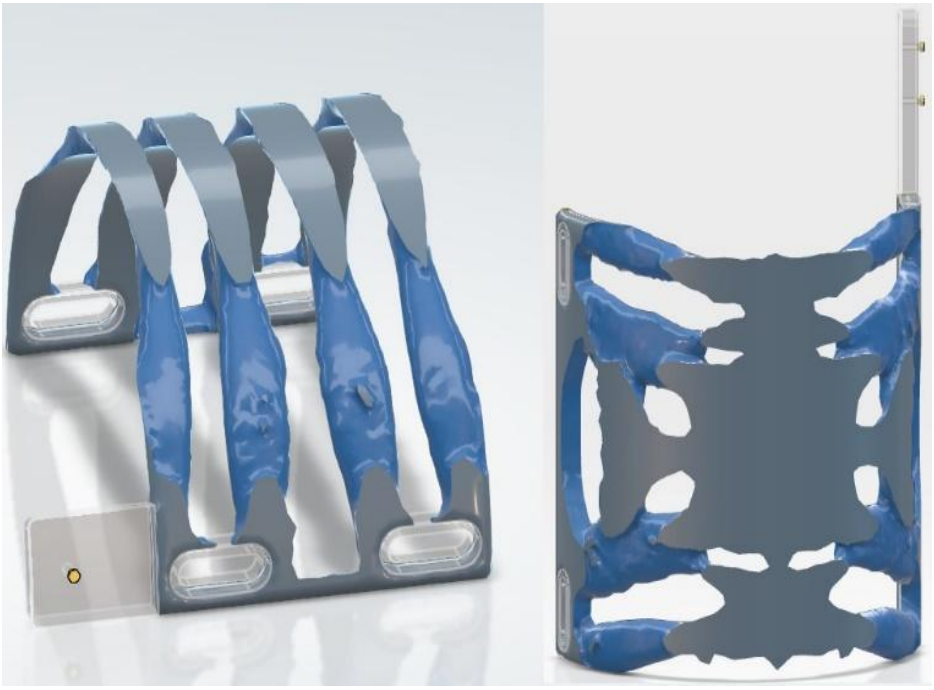

Figure 2. Proposed prototypes of thigh (left) and shin (right) brace.

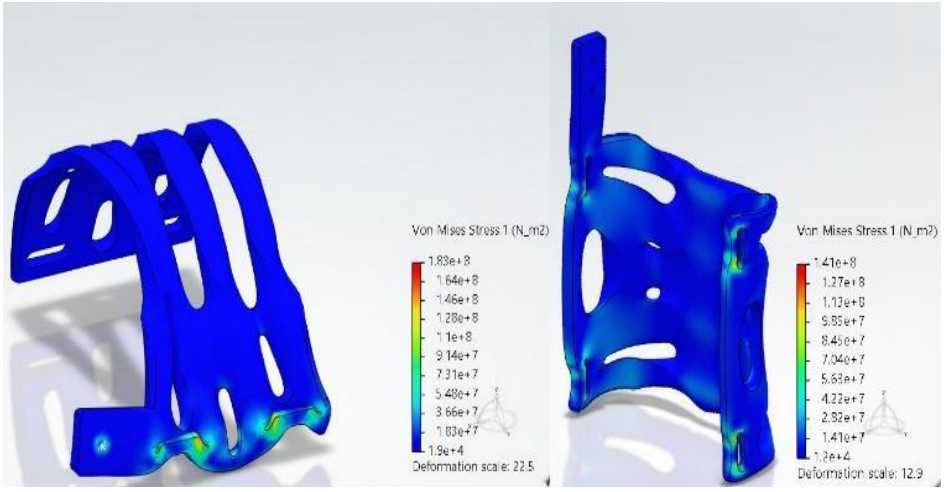

Figure 3. Von Mises stresses experienced by conceptual shapes of thigh (left) and shin (right) brace.

Figure 3 shows the same loads applied on the conceptual cases with a 50% mass constraint after optimisation. This mass constraint led to the optimised thigh brace having a new mass of 0.08kg,

 doi:10.20944/preprints202507.0892.v1

resulting in an approximate 0.051kg weight reduction; and the optimised shin brace having a new mass of 0.137kg, resulting in an approximate 0.062kg weight reduction, which helped to provide definite benefits in terms of wearer comfort and mobility. Because it lessens fatigue and improves the brace's wearability, this reduction is especially important for sportsmen or recuperating patients performing repetitive exercises. Additionally, the 50% mass constraint models' von Mises stress increased by approximately twofold according to finite element calculations, indicating a less effective stress distribution throughout the modified lattice structure. This was a surprising but positive result, showing that the generative method redistributed material under more stringent mass limitations, lowering critical stress concentrations without sacrificing performance as shown in Table 1 below

Table 1. Simulated Output Parameters of Braces.

Braces and Mass Constraints	Mass (kg)	Von Mises Stress (Nm^2)	Displacement (mm)	Score
Thigh, 100%	0.131	5.37×10^9	0.94	—
Thigh, 50%	0.080	1.87×10^8	0.84	60.87
Thigh, 45%	0.071	1.98×10^8	1.22	65.87
Thigh, 40%	0.062	2.45×10^8	2.99	43.91
Shin, 100%	0.199	4.81×10^7	0.46	—
Shin, 50%	0.137	1.41×10^8	1.48	57.31
Shin, 45%	0.122	1.58×10^8	1.83	54.38
Shin, 40%	0.109	1.83×10^8	2.16	39.13

In wearable orthoses, higher displacement is undesirable as it can result in localized deformation during impact, potentially causing discomfort or injury if the brace presses into the user's skin. Therefore, maintaining lower displacement values is essential to ensure both comfort and safety. Trade-off studies were tabulated in Table 1 for the thigh brace and shin brace, and mass constraints of 40%, 45%, and 50% were evaluated to understand the balance between weight savings and structural performance. Results from the original models were also tabulated in the same table. Trade off study scores out of 100 were used to determine the best mass constraints for both braces, with the same input load being used from Figure 1's simulations. Mass constraints below 40% were avoided to prevent excessive material removal that could compromise the overall stiffness and structural integrity of the brace. While lower mass improves mobility and reduces fatigue, a minimum threshold is needed to preserve the mechanical robustness required for repeated dynamic use.

Following these results, a graph of the reduction in weight for both the base models and optimised models is shown in Figure 4.

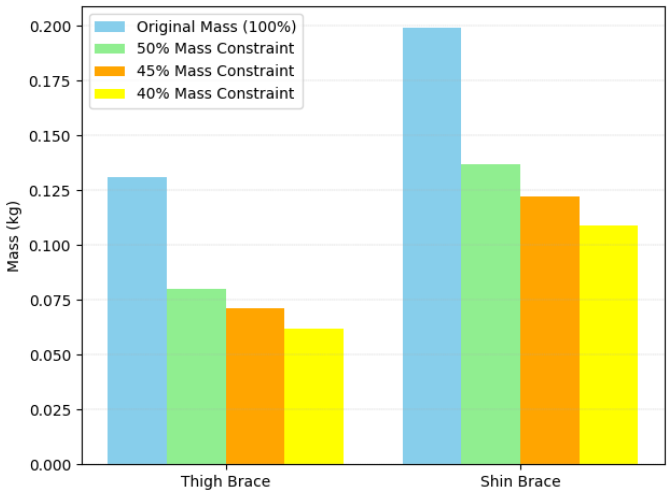

 doi:10.20944/preprints202507.0892.v1

Figure 4. Comparison of Thigh and Shin Braces with Varying Mass Constraints.

Overall, although the 50% mass constraint design for the shin brace was slightly stiffer, it showed that higher stress levels could cause discomfort or shorten its lifespan when subjected to repeated loading. The 45% model for the thigh brace, on the other hand, is a better choice for dynamic use cases, such athletic therapy or later-stage recovery involving frequent mobility, as its minor weight decrease is balanced by its enhanced stress management and structural durability. The final design was 3D-printed with PLA and was physically tested on a user's leg to validate fit and function. To connect the knee brace and shin brace together, a hinge was 3D-printed with a maximum angle of rotation of 105°. The brace shown in Figure 5 successfully aligned with anatomical landmarks, and the hinge system operated smoothly during flexion. The user reported comfort and adequate support without restriction, confirming the effectiveness of the topologically optimized structure. These results support knee orthosis as a viable, ergonomic solution for athletic rehabilitation and daily wear.

Figure 5. Final 3D-printed prototype testing.

3. Discussion

The final knee brace design was selected following extensive simulation and trade-off analysis, optimizing for mass reduction, structural integrity, and stress tolerance. The thigh brace implemented a 45% mass constraint, while the shin brace adopted a 50% constraint, together resulting in a combined material weight of 0.208kg, a reduction in weight of 36.97% compared to the combined weight of the original model (0.330kg) in Figure 5. This reduced the total prototype weight by approximately 63 grams and significantly lowered material usage, yielding tangible cost savings in 3D printing. While designs with more aggressive material removal offered additional weight reductions, they introduced higher stress concentrations and excessive deformation, making them unsuitable for rehabilitation use. Conversely, less optimized models-maintained strength but failed to deliver the desired efficiency gains. Practical considerations such as hinge alignment and printability also influenced the final configuration. Although topology optimization generated high-performance geometries, certain features, such as thin overhangs and unsupported cavities, posed challenges during printing. These issues required minor geometric adjustments and careful print orientation to minimize support structure usage and reduce damage risk during post-processing. This iterative refinement process underscored the importance of integrating design-for-manufacturing principles early in development, especially when engineering orthotic components where material efficiency, cost, and structural performance must be carefully balanced.

4. Conclusion

This proposed work successfully demonstrated the use of Functional Generative Design in combination with 3D-printing to create a lightweight, structurally efficient knee brace for sports rehabilitation. The final prototype balanced material efficiency, mechanical performance, and user

 doi:10.20944/preprints202507.0892.v1

functionality, though challenges with geometry complexity and printability were noted. While the design met many objectives, future improvements, such as integrating patient-specific scans, exploring alternative materials, and conducting mechanical testing, could enhance customization and validation. The study highlights the potential of simulation-driven design and additive manufacturing for developing personalized, eco-friendly orthotic solutions. Using PLA supports sustainability, and expanding the brace to support the entire leg could further improve injury prevention and rehabilitation. Overall, this work showcases how combining generative design with material science can drive innovation in accessible and effective orthopedic devices.

References

1. Zhou, M., Sun, C., Naghavi, S. A., Wang, L., Tamaddon, M., Wang, J., & Liu, C. (2024, February). The design and manufacturing of a Patient-Specific wrist splint for rehabilitation of rheumatoid arthritis. Materials & Design, 238, 1-12. 10.1016/j.matdes.2024.112704.
2. Srikanth, S. A., & Bharanidaran, R. (2017, June). Design of a compliant mechanism based prosthetic foot. International Journal of Mechanical and Production, 7(3), 33-42.
3. Steck, P., Scherb, D., Witzgall, C., Miehling, J., & Wartzack, S. (2023, May 2). Design and Additive Manufacturing of a Passive Ankle–Foot Orthosis Incorporating Material Characterization for Fiber-Reinforced PETG-CF15. Additive Manufacturing of Composites, Volume II, 1-17. 10.3390/ma16093503.
4. Rajput, S., Burde, H., Singh, U. S., Kajaria, H., & Bhagchandani, R. K. (2021). Optimization of prosthetic leg using generative design and compliant mechanism. 3rd International Conference on Materials, Manufacturing and Modelling, 46(17), 8708-8715. 10.1016/j.matpr.2021.04.026.
5. Yan, W., Ding, M., Kong, B., Xi, X., & Zhou, M. (2019, July 13). Lightweight Splint Design for Individualized Treatment of Distal Radius Fracture. Journal of Medical Systems, 43, 1-10. 10.1007/s10916-019-1404-4.
6. Cazon, A., Kelly, S., Paterson, A. M., Bibb, R. J., & Campbell, R. I. (2017, July 8). Analysis and comparison of wrist splint designs using the finite element method: Multi-material three-dimensional printing compared to typical existing practice with thermoplastics. Journal of Engineering in Medicine, 231(9). 10.1177/0954411917718221.
7. Singer, J. C., & Lamontagne, M. (2008, January). The effect of functional knee brace design and hinge misalignment on lower limb joint mechanics. Clinical Biomechanics, 23(1), 52-59. 10.1016/j.clinbiomech.2007.08.013.
8. Robert Lachaine, X., Dessery, Y., Belzile, É. L., & Corbeil, P. (2022, July). Knee braces and foot orthoses multimodal treatment of medial knee osteoarthritis. Gait & Posture, 96, 251-256. 10.1016/j.gaitpost.2022.06.004.
9. Briard, T., Segonds, F., & Zamariola, N. (2020, August 3). G-DfAM: a methodological proposal of generative design for additive manufacturing in the automotive industry. International Journal on Interactive Design and Manufacturing (IJIDeM), 14, 875-886. 10.1007/s12008-020-00669-6.
10. Cho, J.-E., Seo, K.-J., Ha, S., & Kim, H. (2023). Effects of community ambulation training with 3D-printed ankle–foot orthosis on gait and functional improvements: a case series of three stroke survivors. Frontiers in Neurology, 14, 1-9. 10.3389/fneur.2023.1138807.
11. Oka, T., Wada, O., Asai, T., Maruno, H., & Mizuno, K. (2020). Importance of knee flexion range of motion during the acute phase after total knee arthroplasty. Physical Therapy Research, 23(2), 143-148. 10.1298/ptr.E9996.
12. Farah, S., Anderson, D. G., & Langer, R. (2016, December 15). Physical and mechanical properties of PLA, and their functions in widespread applications — A comprehensive review. Advanced Drug Delivery Reviews, 107, 367-392. 10.1016/j.addr.2016.06.012.
13. Vukasovic, T., Vivanco, J. F., Celentano, D., & García-Herrera, C. (2019, August 8). Characterization of the mechanical response of thermoplastic parts fabricated with 3D printing. The International Journal of Advanced Manufacturing Technology, 104, 4207-4218. 10.1007/s00170-019-04194-z.
14. Kok, C.L.; Dai, Y.; Lee, T.K.; Koh, Y.Y.; Teo, T.H.; Chai, J.P. A Novel Low-Cost Capacitance Sensor Solution for Real-Time Bubble Monitoring in Medical Infusion Devices. Electronics 2024, 13, 1111. doi: 10.3390/electronics13061111

 doi:10.20944/preprints202507.0892.v1

15. García-Ávila, J.; Rodríguez, C.A.; Vargas-Martínez, A.; Ramírez-Cedillo, E.; Martínez-López, J.I. E-Skin Development and Prototyping via Soft Tooling and Composites with Silicone Rubber and Carbon Nanotubes. Materials 2021, 15, 256.
16. Klute, G. K., C. F. Kallfelz, and J. M. Czerniecki, Mechanical properties of prosthetic limbs: adapting to the patient. J Rehabil Res Dev, 2001. 38(3): p. 299-307
17. Fey, N. P., A. K. Silverman, and R. R. Neptune, The influence of increasing steady-state walking speed on muscle activity in below-knee amputees. J Electromyogr Kinesiol, 2009.
18. Rogati, G.; Caravaggi, P.; Leardini, A. Design principles, manufacturing, and evaluation techniques of custom dynamic ankle-foot orthoses: A review study. J. Foot Ankle Res. 2022, 15, 38.
19. Rossetos, I.; Gantes, C.J.; Kazakis, G.; Voulgaris, S.; Galanis, D.; Pliarchopoulou, F.; Soultanis, K.; Lagaros,N.D. Numerical Modeling and Nonlinear Finite Element Analysis of Conventional and 3D-Printed SpinalBraces. Applied Sciences 2024,14, 1735. Number: 5 Publisher: Multidisciplinary Digital Publishing Institute, doi:10.3390/app14051735.
20. Witzgall, C.; Völkl, H.; Wartzack, S. Derivation and Validation of Linear Elastic Orthotropic Material Properties for Short Fibre Reinforced FLM Parts. J. Compos. Sci. 2022, 6, 101.
21. R. Bharanidaran and S. A. Srikanth, "A new method for designing a compliant mechanism-based displacement amplifier," in IOP Conference Series: Materials Science and Engineering, 2016, vol. 149, no.1.
22. C. L. Kok, T. H. Teo, Y. Y. Koh, Y. Dai, B. K. Ang and J. P. Chai, "Development and Evaluation of an IoT-Driven Auto-Infusion System with Advanced Monitoring and Alarm Functionalities," 2024 IEEE International Symposium on Circuits and Systems (ISCAS), Singapore, Singapore, 2024, pp. 1-5, doi: 10.1109/ISCAS58744.2024.10558602.
23. Zhang, Y.; Liang, J.; Xu, N.; Zeng, L.; Du, C.; Du, Y.; Zeng, Y.; Yu, M.; Liu, Z. 3D-printed brace in the treatment of adolescent idiopathic scoliosis: a study protocol of a prospective randomised controlled trial. BMJ Open 2020,10, e038373. Publisher: British Medical Journal Publishing Group Section: Surgery, doi:10.1136/bmjopen-2020-038373.
24. Redaelli, D.F.; Abbate, V.; Storm, F.A.; Ronca, A.; Sorrentino, A.; De Capitani, C.; Biffi, E.; Ambrosio, L.;Colombo, G.; Fraschini, P. 3D printing orthopedic scoliosis braces: a test comparing FDM with thermoforming. Int J Adv Manuf Technol 2020,111, 1707–1720.
25. Frangedaki, E.; Sardone, L.; Marano, G.C.; Lagaros, N.D. Optimisation-driven design in the architectural, engineering and construction industry. Proceedings of the Institution of Civil Engineers - Structures and Buildings2023,176, 998–1009, [https://doi.org/10.1680/jstbu.22.00032]. doi:10.1680/jstbu.22.00032
26. Scherb, D.; Steck, P.; Wartzack, S.; Miehling, J. Integration of musculoskeletal and model order reduced FE simulation for passive ankle foot orthosis design. In Proceedings of the 27th Congress of the European Society of Biomechanics, Porto, Portugal, 26–29 June 2022.
27. Mayer, J.; Wartzack, S. Computational Geometry Reconstruction from 3D Topology Optimization Results: A New Parametric Approach by the Medial Axis. Comput. Des. Appl. 2023, 20, 960–975.
28. Andreassen, E.; Clausen, A.; Schevenels, M.; Lazarov, B.; Sigmund, O. Efficient topology optimization in MATLAB using 88 lines of code. Structural and Multidisciplinary Optimization 2011,43, 1–16.doi:10.1007/s00158-010-0594-7.
29. Wang, Xiaojian, et al. "Topological design and additive manufacturing of porous metals for bone scaffolds and orthopedic implants: a review." Biomaterials 83 (2016): 127-141.
30. Kok, C.L.; Tan, T.C.; Koh, Y.Y.; Lee, T.K.; Chai, J.P. Design and Testing of an Intramedullary Nail Implant Enhanced with Active Feedback and Wireless Connectivity for Precise Limb Lengthening. *Electronics* 2024, *13*, 1519.
31. Agache PG, Monneur C, Leveque JL, Rigal JD (1980) Mechanical proper-ties and young's modulus of human skin in vivo. Archives of Dermatological Research 269(3):221–232, DOI 10.1007/BF00406415
32. Wohlers, T., Campbell, R. I., Huff, R., Diegel, O., & Kowen, J.: Wohlers report 2019: 3D printing and additive manufacturing state of the industry. Wohlers Associates (2019)
33. Chew KTL, Lew HL, Date E, Fredericson M (2007) Current evidence and clinical applications of therapeutic knee braces. American Journal of Physical Medicine & Rehabilitation 86(8):678–686, DOI 10.1097/PHM.0b013e318114e416

 doi:10.20944/preprints202507.0892.v1

34. Bethke K (2005) The second skin approach: skin strain field analysis and mechanical counter pressure prototyping for advanced spacesuit design. Thesis, Massachusetts Institute of Technology
35. Diridollou S, Black D, Lagarde J, Gall Y, Berson M, Vabre V, Patat F, VaillantL (2000) Sex- and site-dependent variations in the thickness and mechanical properties of human skin in vivo. International Journal of Cosmetic Science22(6):421–435, DOI 10.1111/j.1468-2494.2000. 00037.x
36. Kok, C.L.; Ho, C.K.; Teo, T.H.; Kato, K.; Koh, Y.Y. A Novel Implementation of a Social Robot for Sustainable Human Engagement in Homecare Services for Ageing Populations. Sensors 2024, 24, 4466. doi: 10.3390/s24144466
37. Kuo, T.C., Huang, S.H., Zhang, H.C.: Design for manufacture and design for 'X': concepts, applications, and perspectives. Comput. Ind. Eng. 41(3), 241–260 (2001)
38. Laverne, F., Segonds, F., Anwer, N., et al.: Assembly based methods to support product innovation in design for additive manufacturing: an exploratory case study. J. Mech. Des. 137, 121701 (2015)
39. Molimard J, Navarro L (2013) Uncertainty on fringe projection technique: a Monte-Carlo-based approach. Optics and Laser in Engineering 51(7):840–847
40. Guo, X., Zhang, W., Zhang, J., et al.: Explicit structural topology optimization based on moving morphable components (MMC) with curved skeletons. Comput. Methods Appl. Mech. Eng. 310, 711–748 (2016)
41. Deckers JP, Vermandel M, Geldhof J, Vasiliauskaite E, Forward M, PlasschaertF. Development and clinical evaluation of laser-sintered ankle foot orthoses. Plastics Rubber Composites. (2018) 47:42–6. doi: 10.1080/14658011.2017.14137608.
42. J. Kong, L. Siek and C. L. Kok, "A 9-bit body-biased vernier ring time-to-digital converter in 65 nm CMOS technology," 2015 IEEE International Symposium on Circuits and Systems (ISCAS), Lisbon, Portugal, 2015, pp. 1650-1653, doi: 10.1109/ISCAS.2015.7168967.
43. Wimmer MA, Nechtow W, et al.: Knee flexion and daily activities in patients following total knee replacement: a comparison with ISO standard 14243. Biomed Res Int. 2015 Aug 11. doi :10.1155/2015/157541.
44. Jørgensen HS, Nakayama H, R aaschou HO, Olsen TS. Recovery of walking function in stroke patients: the Copenhagen Stroke Study. Arch Phys Med Rehabil. (1995) 76:27–32. doi: 10.1016/S0003-9993(95)80038-72.
45. Silva SM, Corrêa JCF, Pereira GS, Corrêa FI. Social participation following a stroke: an assessment in accordance with the international classification of functioning, disability and health. Disabil Rehabil. (2019) 41:879–86. doi: 10.1080/09638288.2017.141342817.
46. Ebert JR, Munsie C, et al.: Guidelines for the early restoration of active knee flexion after total knee arthroplasty: implications for rehabilitation and early intervention. Arch Phys Med Rehabil.2014; 95: 1135-1140.
47. Jakobsen TL, Christensen M, et al.: Reliability of knee joint range of motion and circumference measurements after total knee arthroplasty: does tester experience matter? Physiother ResInt. 2010; 15: 126-134
48. Hesse S, Werner C, Matthias K, Stephen K, Berteanu M. Non–velocity-related effects of a rigid double-stopped ankle-foot orthosis on gait and lower limb muscle activity of hemiparetic subjects with an equinovarus deformity. Stroke. (1999) 30:1855–61. doi: 10.1161/01.STR.30.9.1855
49. Bangor A, Kortum PT, Miller JT. An empirical evaluation of the system usability scale. Intl J Hum Comp Int. (2008) 24:574–94. doi: 10.1080/10447310802205776
50. Gatha NM, Clarke HD, et al.: Factors affecting postoperative range of motion after total knee arthroplasty. J Knee Surg. 2004;17: 196-202.